Growth and magnetism of Co films on a Pd monolayer on Cu(001)

Y. F. Lu,[1,2] M. Przybylski,[1,3,*] M. Nývlt,[1,4] A. Winkelmann,[1] L. Yan,[1] Y. Shi,[1] J. Barthel,[1] and J. Kirschner[1]
[1]*Max-Planck Institut für Mikrostrukturphysik, Weinberg 2, 06120 Halle (Saale), Germany*
[2]*Northwest Institute for Non-Ferrous Metal Research, PO 51, 710016, Xi'an, People's Republic of China*
[3]*Solid State Physics Department, Faculty of Physics and Applied Computer Science, AGH University of Science and Technology, Mickiewicza 30, 30-059 Krakow, Poland*
[4]*Faculty of Mathematics and Physics, Institute of Physics, Charles University, Ke Karlovu 5, 12116 Praha 2, Czech Republic*
(Received 24 May 2005; revised manuscript received 29 November 2005; published 25 January 2006)

We have grown epitaxial Co films on single monolayers (ML) of Pd on Cu(001) substrates at room temperature. The interlayers of Pd were grown by pulsed laser deposition whereas the Co films were prepared by thermal deposition. A layer-by-layer growth mode of Co on the 1 ML Pd/Cu(001) system continues up to at least 11 ML of Co in contrast to the 4 ML of Co on the Pd(001) substrate. This is due to a reduced lattice mismatch for the Co films on the Pd/Cu(001) system in comparison to the Co films on the Pd(001) substrate. On the basis of magneto-optical Kerr rotation data we discuss the effect of the Co-Pd interface contribution to magnetism and to the magneto-optical response.

DOI: 10.1103/PhysRevB.73.035429 PACS number(s): 78.20.Ls, 75.70.Cn, 75.70.Ak

I. INTRODUCTION

For many years, artificial heteroepitaxial Co films adjacent to nonmagnetic metals have been intensively studied due to their importance for technical applications in magnetic or magneto-optical recording devices. In these low-dimensional systems grown on nonmagnetic metal substrates, the structure and magnetism of Co films are different from those of bulk Co due to reduced dimensionality. Symmetry breaking together with magnetic interaction at ferromagnetic/nonferromagnetic metal interfaces play a key role.[1] Enhanced moment and desired magnetic anisotropy could be therefore obtained in ultrathin or multilayer films in a controllable way.

The Co/Cu heterostructures including single and multilayer films have been intensively investigated since the discovery of the oscillatory magnetic interlayer coupling[2,3] and the giant magnetoresistance.[4] In general, it has been accepted that ultrathin fcc Co films grow epitaxially on Cu(001) in a layer-by-layer mode for thicknesses larger than 2 monolayers (ML). Deviations from the ideal layer-by-layer growth in the regime of coverage below two monolayers were observed.[5] The interface strain induced by the lattice mismatch of 1.9% and the substrate topology strongly influence the magnetic properties of the Co films.[6,7] Stepanyuk *et al.*[8] have proposed the concept of mesoscopic misfit to determine the atomistic process in the early stages of heteroepitaxial growth as an example for Co on Cu(001). As a prototype system for intermixing during heteroepitaxy, Co on Cu(001) has been theoretically studied recently by several groups. Pentcheva *et al.*[9] have suggested that a pronounced deviation from the typical Arrhenius behavior of island growth could be attributed to activation of atomic exchange pinning at substitutional Co and aggregation of Cu adatoms. With the help of static energy calculations and accelerated molecular dynamics simulations Miron *et al.*[10] have successfully dealt with the upward interlayer transport mechanism contributing to bilayer island formation at low surface coverage and temperature.

Bulk Co crystals have a hcp structure and a Curie temperature of 1395 K. The magnetic moment per atom is $1.72\mu_B$ and the easy axis of magnetization points along the *c* axis of the hcp structure. The well-known hcp-fcc phase transition of Co occurs at 690 K. At room temperature, the hcp and fcc phases can coexist in thin films because of the small energy difference between the two phases. Co films of metastable fcc structure can be deposited on properly chosen substrates at low temperatures. This is the case for ultrathin Co films grown on Cu(001) and Pd(001) substrates. The structure and magnetic properties of Co films on Cu(001) below 2 ML have attracted significant interest. A sudden jump of the Curie temperature at a critical coverage between 1 and 2 ML, where a metastable magnetic phase related to the island coalescence exists, has been observed, indicating a strong correlation between magnetism and structure in ultrathin Co films.[11] Recent experimental results have also confirmed this point.[12–15]

In case of Co/Pd thin films and multilayer systems, the existence of perpendicular magnetic anisotropy and of enhanced magnetic moments have attracted much attention.[16–18] Theoretical calculations have predicted that giant magnetic moments of 3*d* impurities in the Pd host would appear due to the induced spin polarization in Pd which has a stronger spin-orbit coupling than Co.[16] At palladium-ferromagnet interfaces, the first Pd layer could acquire a magnetic moment of about $0.3\mu_B$ per Pd atom, which would then decay rapidly with distance from the interface.[17] Some experimental efforts based on the x-ray magnetic circular dichroism (XMCD) technique have been applied to study enhanced orbital magnetic moments of Co atoms in Co/Pd multilayers[18] and Pd/Co/Pd trilayers[19] where the hybridization of interfacial Co and Pd plays a key role. Very recently, Imai *et al.* have developed a theoretical model for the temperature dependent magnetic properties for Co/Pd multilayer thin films.[20] Their results have shown the importance of the exchange coupling at the Co-Pd interface. However, very few investigations on ultrathin Co films on Pd(001) substrates have been reported. The relatively large mismatch of

9.8% (a_{Co}=3.54 Å, a_{Pd}=3.89 Å) between the bulk lattice of fcc Co and Pd greatly influences the growth and structure of the Co films.

In order to verify experimentally the hypothesis of enhanced magnetic moments at the Co-Pd interface and the spatial extent of the Co-Pd interaction, the Co/Pd system should be compared with identical Co films grown on a nonferromagnetic substrate with a very small spin-orbit coupling. As mentioned above, in ultrathin Co films the structure and magnetism are strongly correlated. Therefore, to obtain reasonable results from such a comparison, it is necessary to eliminate structural effects induced in the Co films by different substrates. In the following, we will show how this requirement can be met by using the same nonferromagnetic substrate either without or with an ultrathin Pd buffer layer. To avoid the large lattice mismatch, it is very useful to grow the Co films (and the Pd buffer layer) on a substrate having the lattice constant similar to that of Co. A good candidate is Cu(001) which has a mismatch with the fcc Co(001) of 1.9% only.

The aim of this paper is to compare the Co films grown on the Cu(001) surfaces to the Co films grown on epitaxial Pd buffer layers prepared on the Cu(001) substrates. It will be shown that the ultrathin Pd film adjusts its in-plane lattice constant to fit that of the Cu(001) surface. Consequently, the Co films grown directly on Cu(001) and on the Pd(001) buffer on Cu(001) have almost the same crystallographic structure. By varying the thickness of the Pd buffer layer, we will show how the insight can be gained into the Co/Pd interface magnetism, especially into the spatial extension of the Co-Pd electronic hybridization.

II. EXPERIMENTAL PROCEDURES

Few-monolayers-thick Pd films on Cu(001) were grown by the pulsed laser deposition (PLD) method in a multichamber ultrahigh vacuum system with a base pressure $<5\times10^{-11}$ mbar and with the pressure less than 2×10^{-10} mbar during deposition. The Cu(001) substrate was cleaned by cycles of Ar^+ sputtering followed by annealing at 900 K until only the Cu lines in the Auger electron spectra appeared and sharp low energy electron diffraction (LEED) spots together with atomically smooth terraces under a scanning tunneling microscope (STM) were observed. During the deposition, the substrate was placed about 100–130 mm away from the Pd source target and its temperature was kept at 300 K. In the case of PLD, the KrF excimer laser (248 nm wavelength) pulse energy was set to 325 mJ. All Co films were prepared by thermal deposition (TD). The whole growth process of the films was monitored by a reflection high energy electron diffraction (RHEED) system. All STM measurements were performed in a constant current mode at 0.2–0.5 V positive tip bias voltage and 0.1–0.5 nA tunneling current. The magnetic properties were studied by using the longitudinal and polar magneto-optical Kerr effects (MOKE) where a *p*-polarized laser beam with a wavelength of 675 nm (i.e., with the photon energy of 1.84 eV) was used. The *p* polarization was set by using a Glan-Thompson polarizer which stops the weak *s*-polarized part of the laser beam. For the longitudinal MOKE, the incidence angle (with respect to the surface normal) of the probing laser beam was $68°\pm2°$. For the polar MOKE, the incidence angle was approximately 5° (nearly normal incidence). The errors in determination of the angle of incidence originate mainly from the mechanical restrictions imposed by the electromagnet. After reflection from the sample surface the laser beam passed the elasto-optical modulator working at the frequency $\omega_m\approx50$ kHz, with principal axes parallel approximately to the *p* and *s* directions. After passing the modulator the laser beam entered an analyzer with the polarization axis oriented at 45° with respect to the *p* (or *s*) direction. The laser beam transmitted by the analyzer was detected by a photodiode and the signal was analyzed by a lock-in amplifier. The signal component oscillating at the $2\omega_m$ frequency is a linear function of the Kerr rotation angle of the specimen. The difference of two $2\omega_m$ signals measured in magnetic saturation for two opposite orientations of magnetization vector in longitudinal or in polar magneto-optical geometry is then proportional to the Kerr rotation angle of the studied specimen. The rotation angle is calibrated by measuring the $2\omega_m$ signal change corresponding to rotation of the polarizer from the *p* direction by a well-defined very small angle.

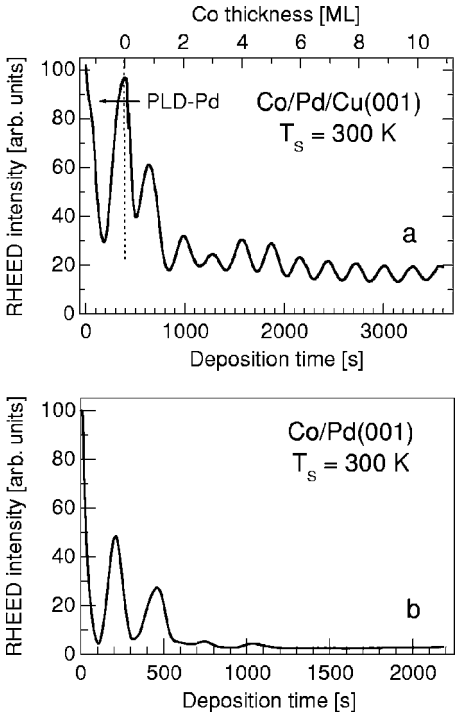

FIG. 1. RHEED intensity oscillations vs time during deposition of Co on the 1-ML-thick Pd buffer layer grown on Cu(001) (a) and on Pd(001) (b). The monolayer of Pd was grown by PLD, whereas the Co films were thermally deposited at room temperature. RHEED during film growth was performed at a glancing angle of approximately 3° and an electron energy of 35 keV.

III. RESULTS

Figure 1 shows the RHEED intensity of the specular spot as a function of deposition time for the Pd buffer and the Co

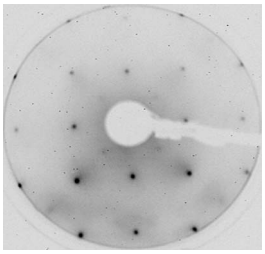

FIG. 2. LEED pattern of 1 ML of Pd on Cu(001). The image was taken at 165 eV beam energy. Only very weak $c(2\times2)$ spots show up after strong contrast enhancement.

layer on the Cu(001) substrate [Fig. 1(a)] and for the Co layer on the Pd(001) substrate [Fig. 1(b)], both deposited at room temperature. The RHEED intensities are normalized to their initial values before starting the deposition process. After 1 ML of the pulsed-laser-deposited Pd buffer the RHEED intensity recovers almost to the same level as for the Cu(001), indicating an extremely small surface roughness. This observation agrees with our STM results, as will be discussed later. The smooth Pd interlayer provides a layer-by-layer epitaxy of forthcoming Co layers. Clear RHEED oscillations up to at least 11 ML of the Co film thickness [Fig. 1(a)] indeed confirm this point.

For the Co/Pd(001) films [Fig. 1(b)], only two initial oscillations are clearly observed. This indicates a three-dimensional character of growth above 2 ML. The third and fourth oscillations in the specular RHEED intensity are still visible, but their amplitudes are very small. From the RHEED intensity oscillations the deposition time for 1 ML of Co is estimated to be 288 s on the Pd/Cu(001) system, and 250 s on the Pd(001) substrate. The ratio of deposition times for one monolayer of Co is 1.15. This means that the Co atomic density on the Pd/Cu(001) system is larger than that on the Pd(001) substrate. It should be noted that both depositions were made under identical conditions, and at exactly the same distance between the sample and the evaporator. The Co deposition rate was calibrated in the beginning as well as at the end of the experiment with equal results.

In Fig. 2, the LEED pattern of 1 ML Pd on Cu(001) deposited by PLD shows a clear $p(1\times1)$ structure. This proves pseudomorphic growth of the Pd film, despite there is the relatively large lattice misfit of 7.8% between Cu (a_{Cu} =3.61 Å) and Pd (a_{Pd}=3.89 Å). For the PLD grown Pd there are no noticeable superstructure spots visible in the recorded LEED pattern. Only very weak $c(2\times2)$ spots show up after strong contrast enhancement. On the contrary, in the case of thermal deposition of Pd on Cu(001), a pronounced $c(2\times2)$ LEED superstructure indicates substantial surface alloying.[21] The suppression of interface alloying in the case of Pd grown by PLD is most likely due to the very high nucleation density. It has been also confirmed by surface x-ray diffraction experiments that for 1.1 ML of PLD-grown Pd on Cu(001) within the uncertainty given by the data analysis procedure more than 90% of the deposited Pd is concentrated in the topmost layer, i.e., almost the whole surface of Cu is covered by Pd atoms.[22] The pseudomorphic growth of Pd on Cu(001) is necessary in order to keep the same lattice mismatch between the Co film and the Pd buffer with that between the Co film and the Cu(001) substrate. The strongly suppressed alloying/intermixing between Pd and Cu allows to relate the modified properties of the forthcoming Co films to the presence of a continuous Pd monolayer between the Cu(001) substrate and the Co film.

Figure 3 shows LEED patterns for the Co films grown on two different surfaces. Upon deposition of Co on the Pd buffer layer on Cu(001), the LEED pattern remains nearly unchanged, as shown in Fig. 3(a) for 1 ML of Co and in Fig. 3(b) for 5 ML of Co. Co films were deposited immediately after the Pd layer was grown on Cu(001). In order to prevent Pd from contamination, we allowed no time delay between Pd and Co deposition. Obviously, the (1×1) structure is still distinguishable, even at a coverage of 11 ML [Fig. 3(c)]. This growth of fcc-Co films on 1 ML Pd/Cu(001) is very similar to that of Co on Cu(001). In addition to a long-range ordering of Co atoms in the Pd/Cu(001) case, this suggests a smooth surface of the 11-ML-thick Co film. On the other hand, for thermally deposited Co films on Pd(001), a $p(1\times1)$ LEED pattern could be seen only below a coverage of about 2–3 ML [Fig. 3(d)]. This thickness range corresponds well to the region where the layer-by-layer growth

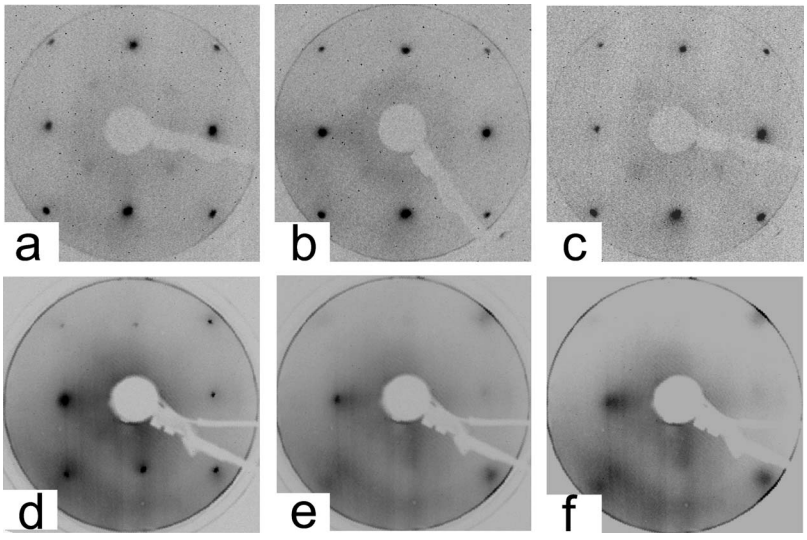

FIG. 3. LEED patterns of Co on 1 ML Pd/Cu(001) for Co thickness of: (a) 1, (b) 5, (c) 11 ML. LEED patterns of Co on Pd(001) for Co thickness of: (d) 2, (e) 4, and (f) 8 ML. The images were taken at 78 eV beam energy.

mode is seen in the RHEED intensity oscillations. With increasing Co thickness the LEED pattern changes very rapidly into a blurred one with a strong diffuse background as seen in Figs. 3(e) and 3(f) for, respectively, 5 and 8 ML of Co on Pd(001). This can be explained by a three-dimensional growth mode above the Co thickness of 2 ML.

At the initial stages of growth, the pulsed-laser-deposited Pd on Cu(001) forms monolayer-thick islands. For coverage of 0.5 ML, which corresponds to the first minimum in the RHEED intensity, the occupied area of the islands on the terrace which was calculated from STM topography image, agrees well with the coverage of 0.5 ML determined by RHEED. Moreover, the step edges of Cu substrate have not been changed upon exposing to Pd. Therefore we believe that during PLD growth of Pd on Cu(001) the nucleation and formation of two-dimensional (2D) islands are mostly attributed to Pd atoms. Figure 4(a) displays a STM image of the PLD-Pd film when the RHEED intensity just shows the first maximum. In real space, a fully wetting film together with a few small islands of 1 ML height is observed. This is characteristic for an ideal layer-by-layer growth mode. The morphology of the Cu substrate is not changed upon Pd deposition. On this flat surface of very homogeneous appearance, measurement of vertical layer distances within the accuracy of a conventional STM proves all islands show the layer height characteristic of Pd(001) (nominally 1.94Å). At room temperature, there is still diffusion along the step edges of the relatively small islands (typical size 2–4 nm), and in combination with the finite tip radius the accuracy of the island height measurement is only about 5%. This threshold, however, is small enough to distinguish between the—apparent—Pd layer distance on one hand and Cu or Co layer distances on the other hand. Figure 4(b) shows a STM image of the clean Pd(001) substrate. After thermally depositing the Co film of about 1 ML thickness on the Pd/Cu(001) system [Fig. 4(c)] we can resolve the Pd layer (dark), the first Co layer (gray), and the second Co layer (white). In this case about 92% of the Pd monolayer are covered by the first monolayer of Co, while about 8% of the deposited Co are forming small second layer islands. This confirms the dominating two-dimensional growth mode. A careful inspection of STM line profiles through second layer islands and first layer holes—within the discussed accuracy limits—reveals a small fraction of Pd (layer spacing of 1.94Å) incorporated in the growing Co. This is no longer the case for the 6 ML Co film in Fig. 4(e), where only Co lattice spacing values can be measured. It should be pointed out that for 0.6 ML of Co on the Cu(001) substrate, bilayer islands were previously detected.[15] Therefore, we can conclude that the Pd buffer greatly supports the initial layer-by-layer growth of the Co film. For 1.1 ML of Co on Pd(001), more than 90% of the Pd substrate is covered by the Co atoms. No essential difference is observed between the STM images for the Co films of about 1 ML on Pd/Cu(001) and on Pd(001). With increasing Co thickness the surface morphology indicates a nearly layer-by-layer growth mode for the Co films on Pd/Cu(001), as it is shown in Fig. 4(e) for 6.0 ML of Co. In contrary, for the Co/Pd(001) system the Co film surface is getting more and more rough. The thicker Co films on Pd(001) display a three-dimensional (3D) island growth mode [Fig. 4(f)].

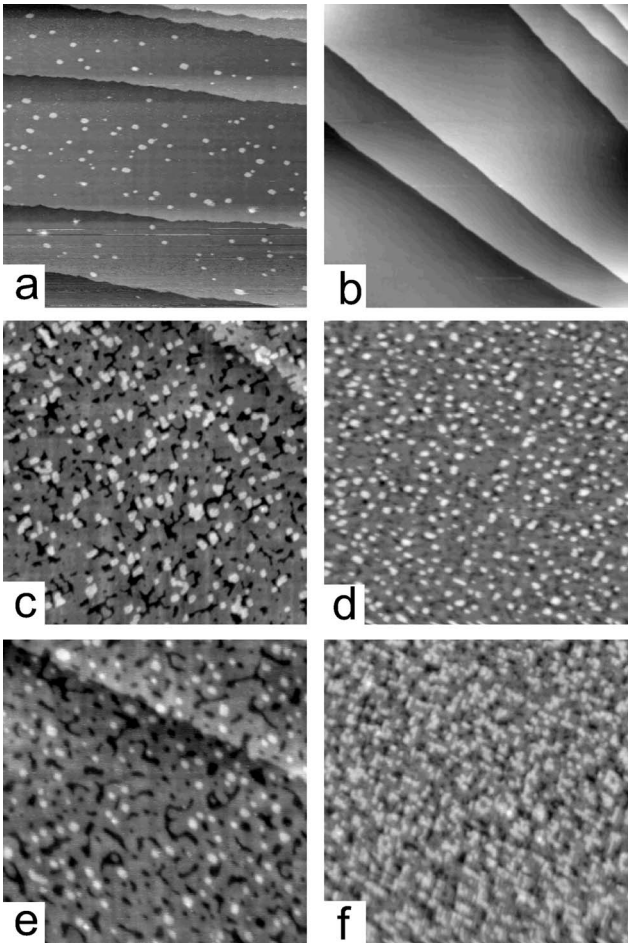

FIG. 4. STM images for (a) 1 ML Pd on Cu(001) substrate (200 nm × 200 nm); (b) clean Pd(001) substrate (500 nm × 500 nm); (c) 1.0 ML of Co on 1 ML of Pd on Cu(001) (100 nm × 100 nm); (d) 1.1 ML of Co on Pd(001) (100 nm × 100 nm); (e) 6.0 ML of Co on 1 ML Pd/Cu(001) (100 nm × 100 nm); and (f) 4.0 ML Co on Pd(001) (100 nm × 100 nm). All Co layers were grown by thermal deposition at room temperature.

We now turn our attention to the magnetism of these systems and further explain its relation to the structure and morphology. Before starting to investigate the Co films on the Pd/Cu(001) system, we will compare the magnetic properties of ultrathin Co films grown on the Cu(001) and on the Pd(001) substrates. Hysteresis loops of these films were measured at 70 K for gradually increasing Co thickness. The external magnetic field was applied along the Co[110] direction. This direction was found to be parallel to the easy axis of magnetization. No polar MOKE signal was detected in the whole Co film thickness range for all systems studied in the present work. The very specific, different experimental conditions required to induce perpendicular magnetic anisotropy in the Co/Pd(001) system are described elsewhere.[23] At 70 K, the Co films exhibited ferromagnetic ordering when the coverage was more than 0.5 ML on both substrates. Figure 5(a) shows the coercivity ($\mu_0 H_C$) of the two systems as a function of the Co thickness. It is seen that nearly in the whole thickness range the coercivity of the Co/Cu(001) is

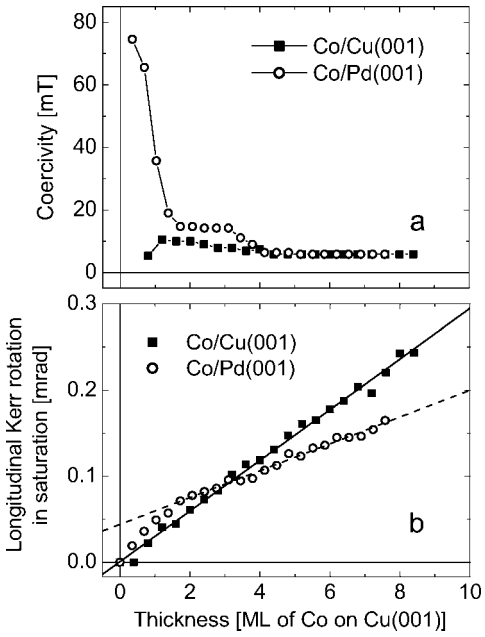

FIG. 5. Thickness dependence of the coercivity (a) and the longitudinal Kerr rotation in magnetic saturation (b) measured along the Co[110] direction at 70 K. The lines serve as guides to the eye.

smaller than that of the Co/Pd(001), especially for the low Co coverage.

Figure 5(b) shows the variation of the longitudinal Kerr rotation with the Co film thickness on both substrates. Because the hysteresis loops are square, the Kerr effect is plotted in remanence in order to minimize the effects of stray magnetic fields on the optical components. In the case of Co/Cu(001), a linear increase of the Kerr rotation signal with Co thickness was observed. In the Co/Pd(001) system, the signal increase below about 2 ML was more rapid than in the Co/Cu(001) system. Above 2 ML, the slope of the dependence on the Co thickness decreased and the Kerr rotation signal varied linearly with the Co thickness. The slope of the linear dependence for the Co/Cu(001) system is obviously much larger than that for Co/Pd(001). From our experimental data plotted in Fig. 5(b) it follows that above 2 ML of Co the ratio of the slopes for Cu and Pd substrates is $\kappa_{\mathrm{exp}}=1.8\pm0.4$. The experimental error is estimated from the expected inaccuracy of setting, measuring and reproducing the angle of incidence for the probing laser beam in the UHV chamber.

An extrapolation of the Kerr rotation signal from the region above 2 ML to zero Co thickness in Fig. 5(b) gives, within our experimental precision, zero for Co on Cu(001). This shows that possible interface contributions can be neglected in this case. On the other hand, a similar procedure applied to the Co films on Pd(001) provides a remarkable offset at zero Co thickness. This offset should originate from a contribution of the Co-Pd interface to the Kerr effect, as will be discussed later in more detail.

It is interesting to compare magnetic properties of the Co/Pd/Cu and the Co/Cu systems where a similar strain state and a layer-by-layer growth mode have been observed, as described above. By such a comparison we try to explore

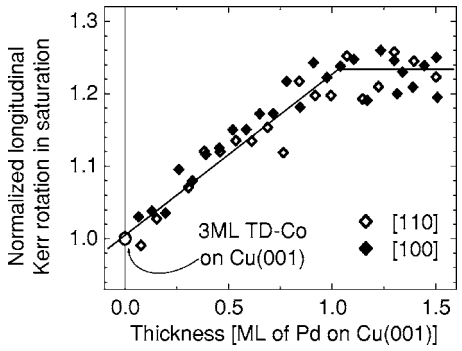

FIG. 6. Pd thickness dependence of Kerr rotation at saturation for 3 ML of Co on the Pd wedge at 70 K. Kerr rotation is normalized to the value of 3 ML thermally deposited Co film on Cu(001). The solid line serves as a guide to the eye.

the role of the Pd interlayer in determining the magneto-optics and the magnetism of these Co layers, in particular to gain some insight into the origin of the offset signal at zero thickness measured in the Co/Pd(001) system. Because of the existence of a metastable phase below a critical coverage $d_c\approx1.8$ ML for Co/Cu(001),[13] we have chosen a 3 ML coverage of Co in order to avoid ambiguities. Figure 6 shows results of the MOKE measurements for 3 ML of Co on a wedge of the Pd interlayer with thickness varying from 0 to 1.5 ML grown on the Cu(001) substrate. Taking into account that the in-plane lattice constant of the pseudomorphic Pd interlayer in the coverage up to 1.5 ML is the same as that of the Cu substrate, the Pd wedge interlayer should not have any additional influence on the strain state and on the structure of 3 ML thermally deposited Co overlayer. Thus, a comparison with 3 ML of Co on Cu(001) is possible, and should be independent of the structure because it is almost identical in both cases. For convenience of comparison the Kerr rotation measured along two directions of [100] and [110] was normalized to the corresponding value on a reference sample of 3 ML Co on Cu(001). We find that the experimental Kerr rotation increases linearly with the Pd interlayer thickness up to 1 ML for both directions. Above 1 ML it stops increasing. The Kerr rotation for a 3-ML-thick Co film on the 1 ML Pd buffer increases by ~20% as compared to the film grown directly on the Cu(001). The same kind of the Pd thickness dependence of the Kerr rotation along two directions shows that the enhanced magneto-optical response is not caused by the change of the magnetic anisotropy. Note that the increase of the Kerr rotation cannot be explained by an increased number of Co atoms because the in-plane lattice spacing of all Co films is determined by the Cu(001) substrate for this Pd buffer thickness range.

In order to clarify the origin of the increased magneto-optical response from the Co/1 ML Pd/Cu(001) in comparison to the Co/Cu(001) specimens, the Kerr rotation was measured for three different thicknesses of the Co film without and with the Pd monolayer between Co and the Cu(001) substrate. The results are shown in Fig. 7. The Kerr rotation signal at every thickness of Co was averaged over at least a 3-mm-long part of the crystal surface perpendicular to the wedge slope so that the error originating from a possible inhomogeneity of the Co film surface or its thickness could

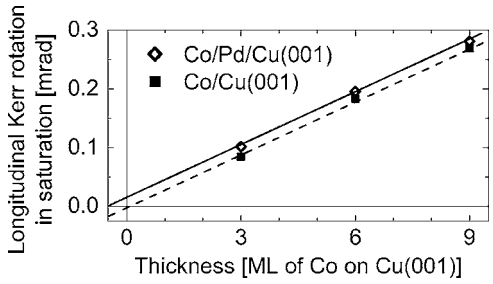

FIG. 7. Comparison of longitudinal Kerr rotation at saturation for Co on 1 ML Pd/Cu(001) and Co on Cu(001) for several Co thicknesses. The MOKE measurement was performed at 70 K. The lines serve as guides to the eye.

be minimized. The saturation Kerr rotation for the Co films grown on 1 ML Pd/Cu(001) is increased in comparison to the films grown on Cu(001) by 20% for 3 ML of Co. Nevertheless, the slope for Co/1 ML Pd/Cu(001) system is exactly the same as for the Co films grown directly on the Cu(001) substrate.

IV. DISCUSSION

First we will discuss the Co growth mode and the structure of the Co/Pd/Cu(001) system. Contrary to the case of the epitaxial growth of Co films on Cu(001) where the first RHEED oscillation peak was missing due to a formation of double-layer islands below 2 ML,[24] we found a real layer-by-layer growth in the Co/Pd/Cu(001) system even during the initial growth stages. According to the simple thermodynamical criterion for heteroepitaxial systems, the layer-by-layer growth is not energetically favored in the case of Co/Cu(001). This follows from considerations of the surface free energy because of the condition $\gamma_{\mathrm{Co}}-\gamma_{\mathrm{Cu}}>\gamma_i$ with $\gamma_{\mathrm{Co}}=2.55\ \mathrm{J\,m^{-2}}$, $\gamma_{\mathrm{Cu}}=1.85\ \mathrm{J\,m^{-2}}$ (Ref. 25), and $\gamma_i=0.25\ \mathrm{J\,m^{-2}}$ (Ref. 26). The existence of a strained Pd interlayer might change the thermodynamical relation in the Co/Pd/Cu(001) system. It seems that a possible larger interface energy could be beneficial to layer-by-layer growth. However, we know only the bulk value for Pd, which is $\gamma_{\mathrm{Pd}}=2.05\ \mathrm{J\,m^{-2}}$.

The difference in the atomic density results from the reduced interatomic distance of Co on Pd/Cu(001) in comparison with that of Co on Pd(001). As long as the coherent epitaxy remains, the Co lattice is forced to keep the lattice constant of the underlying Pd substrate. Therefore, an unequal number of lattice sites has to be occupied to fill 1 ML due to different interatomic spacings. Assuming that the first 2 ML of Co grow pseudomorphic to the substrate in both cases, i.e., on Pd(001) and on the 1 ML Pd/Cu(001) system, we estimate the ratio of the atomic densities to be $a^2_{\text{Co-}on\text{-Pd}}/a^2_{\text{Co-}on\text{-Pd/Cu}}\sim 1.16$. This is very close to the deposition time ratio value of 1.15 for 1 ML of Co on the both surfaces. Therefore, the difference in the deposition time for 1 ML is a result of the Co lattice adjustment to the lattice of the substrate on which the film is growing.

The coercivity of the Co films grown on Pd(001) in the thickness range where the interface is formed is much higher as compared to the coercivity of the Co films grown on Cu(001). The coercivity of the Co/1 ML Pd/Cu(001) is almost the same as for the Co/Cu(001) system. In the Co/Pd(001) system, the Co layer thicker than 2 ML is likely to develop into an unexpanded fcc structure due to the interfacial strain relaxation. During the strain relaxation a number of structural defects (possible domain wall pinning centers) can form, and a long-range crystallographic order is spoilt. This is in agreement with (i) the lack of RHEED oscillations after the second monolayer of Co seen in Fig. 1(b) and (ii) the blur of LEED spots beyond this film thickness [Figs. 3(e) and 3(f)]. For Co on 1 ML Pd/Cu(001), the Co adlayers have a strained structure with much less defects, like in the case of the Co/Cu(001) system.[27] Therefore the coercivity is lower.

The slope of the Co thickness dependent Kerr rotation has shown the importance of the system composition (the substrate and the magnetic film materials) for the magneto-optical response—the difference between the Co/Cu(001) and the Co/Pd(001) systems (Fig. 5), and the similarity between the Co/Pd/Cu(001) and the Co/Cu(001) systems (Fig. 7).

The different slopes of the linear dependence of Kerr rotation on the Co thickness in the Co/Cu(001) [or Co/1 ML Pd/Cu(001)] and in the Co/Pd(001) systems (Fig. 5) can be well explained by the dependence of the magneto-optical response on the substrate material because the film material is the same. When assuming that the optical profile of the interface between the Co film and the nonferromagnetic substrate is steplike and that the Co film is ultrathin (which is well satisfied in our case), one can use approximative expressions for the longitudinal magneto-optical Kerr effect in magnetic films grown on nonferromagnetic substrates. Here we employ the analytical formulas published in Refs. 28–30. When considering that the incident light is *p* polarized, the Kerr rotation on the system writes

$$\theta_K^{(012)}=\Re\left[\frac{2\pi N_0^2 N_2 \sin(2\varphi_0) Q_1 t_1 m_1}{\lambda(N_0\cos\varphi_0+N_2\cos\varphi_2)(N_2\cos\varphi_0-N_0\cos\varphi_2)}\right]. \tag{1}$$

Here $\Re$ indicates the real part, N_0 and N_2 are, respectively, refractive indices of the ambient (vacuum) and the substrate, φ_0 is the angle of incidence of the optical beam with a wavelength λ and φ_2 is the complex angle of refraction in the substrate. Then, t_1 and Q_1 are, respectively, the thickness and the Voigt magneto-optical parameter (i.e., a ratio of the off-diagonal to diagonal permittivity tensor elements) of the ultrathin magnetic film. Finally, m_1 is the relative magnetization of the magnetic film with respect to a complete magnetic saturation in the longitudinal direction (i.e., $m_1=1$ in our case). Equation (1) shows that the Kerr rotation from the Co film should be proportional to the Co film thickness. Even if we consider possible interface effects (e.g., an electronic hybridization or usually expected alloying) which can add some contribution to the Kerr signal, from a certain Co thickness, at which the interface is already stable, the Kerr signal should be changing linearly with the thickness of the Co film. For a given magneto-optical geometry (i.e., the angle of incidence and the incident polariza-

tion), the difference between the slopes of the Kerr rotation signal measured for the Co films grown on Cu(001) and on Pd(001) should originate from different optical properties of Cu and Pd, i.e., from a difference between the values of the refractive index N_2 for Cu and Pd.

We will now compare the experimental ratio of slopes in the Co/Cu(001) and Co/Pd(001) systems, $\kappa_{exp}=1.8\pm0.4$, with theoretical calculations. The Kerr rotation in both systems was calculated by using Eq. (1) with the optical parameters of Cu,[31] of Pd,[32] and Co.[32] The magneto-optical parameter Q_1 was obtained from the experimental Kerr effect on a thick polycrystalline Co film[33,34] and the optical data of Co.[32] The calculated ratio of slopes for Cu and Pd substrates for our photon energy (1.84 eV) is 1.6. When comparing the experimental and theoretical data, it is necessary to bear in mind that the theoretical calculation starts from bulk optical data which can be quite different from those of very clean single crystal surfaces and ultrathin magnetic films. When considering all possible sources of errors, we can conclude that the theoretical calculation reproduces the experimental results in the range above Co thickness of 2 ML very well. This confirms quantitatively that the slopes in this range displayed in Fig. 5(b) should differ because of different substrates used for the Co growth.

In the Co/Pd/Cu(001) system the term $Q_1 t_1 m_1$ in the numerator of the quotient in Eq. (1) will have to be replaced for a saturated longitudinal magnetization ($m_1=1$) by $\int Q_1(t')dt'$ where the integration runs over the Co and Pd layers. This shows that from a certain Co thickness above which the $Q_1(t')$ parameter remains constant the slope of the Kerr rotation variation with the Co film thickness in the systems Co/Pd/Cu(001) and Co/Cu(001) should be identical. This agrees well with the results displayed in Fig. 7.

To explain the dependence of Kerr rotation on the Pd thickness plotted in Fig. 6, one has to consider that at a Pd coverage below 1 ML only a part of the Cu(001) surface is covered with the Pd-monolayer patches. Then the Co film is grown in part on 1 ML Pd/Cu(001) system and in part on the Cu(001) surface. With increasing Pd coverage the fraction of the Co film grown on the islands of 1 ML Pd on Cu(001) increases at the expense of the declining fraction of the Co film grown directly on the clean Cu(001) surface. Thus, the increase of the Kerr rotation with increasing Pd coverage can be well explained by the increasing contribution coming from the Co/1 ML Pd/Cu(001) fraction to the total MOKE signal. Obviously, the saturation Kerr rotation for the Co film grown on the 1 ML Pd/Cu(001) system has to be larger than for the Co film of the same thickness but grown on Cu(001). After the Pd monolayer is completed, the mixture of Co/Cu(001) and Co/1 ML Pd/Cu(001) systems evolves to the homogeneous Co/1 ML Pd/Cu(001) structure. The increased value of the Kerr rotation remains the same when the thickness of the Pd interlayer increases gradually from 1 to 1.5 ML (Fig. 6). This means that the MOKE signal enhancement effect originates at the interface which is "sharp" because it comprises no more than 1 ML of Pd. In our opinion this proves the homogeneity of the Pd monolayer on Cu(001) and the absence of substantial intermixing between Cu and Pd. If we assume a fraction of the deposited Pd incorporated in the subsurface of the Cu substrate, the measured additional Kerr rotation caused by the action of the Co-Pd interface would not saturate already at exactly 1 ML of Pd, but only at a higher Pd coverage when finally a complete Pd monolayer faces the first layer of the growing Co film. The increase of the MOKE signal caused by 1 ML of Pd placed between Co and Cu(001) does not depend on the Co film thickness (Fig. 7) when the Co film is thicker than 1 ML.[35]

We stress the fact that in the case of the 3-ML-thick Co film deposited on Cu(001), a 20% increase of the signal is detected when the same film is deposited on the Pd/Cu(001) system. This means that the contribution to the overall MOKE signal from the Co/Pd interface is equivalent to the contribution from 20% of 3 ML of Co, i.e., 0.6 ML of Co in this case. This is exactly the signal offset at zero thickness of the Co film on Pd/Cu(001)—Fig. 7. This value has to be compared to the signal offset after extrapolation to zero thickness of the Co film grown directly on Pd(001) which is equivalent to the signal from about 2.5 ML of Co—Fig. 5. The signal offset (at zero Co thickness) for the Co/Pd(001) and Co/1 ML Pd/Cu(001) does not have to be the same. One has to remember that the lattice mismatch of 9.8% in the case of Co/Pd(001) is reduced to 1.9% in the case of Co/Pd-monolayer/Cu(001) system. From another point of view, one can imagine that the strained pseudomorphic Pd layer on Cu(001) is trying to relax at the covering by Co. This can support an intermixing between Pd and Co and different magneto-optical properties of the interface. Nevertheless, the resulting signal offset of the Kerr rotation in this case [of unstrained Co films on 1 ML Pd/Cu(001)] is relatively small. Our further (unpublished) experiments with Pd/Co/Cu(001) system show that at reduced Co/Pd intermixing [which is expected in the case of unstrained Co films on Cu(001), covered with Pd], the change of the Kerr rotation due to the Co/Pd interface is even smaller. All these findings together mean that an expansion of the Co lattice seems to play an important role for the increased Kerr rotation from the Co/bulk-Pd interface in comparison to the Co/few ML Pd on Cu(001) interface.

Let us now focus on the enhancement of magnetic moments at the Co-Pd interface. Actually, there is no straightforward reason to conclude on the basis of MOKE studies that the magnetic moments at the Co-Pd interface in the Co/Pd(001) systems are increased with respect to those of Co on the Pd/Cu(001) surface. The Kerr rotation from the Co/Pd interface does not have to scale with the magnetic moment in the same way as for the Co film. This is because, in general, the magneto-optical Voigt parameters Q for the Co film and for the Co/Pd interface are different. Consequently, the increased Kerr rotation cannot be directly related to the magnetic moment of the system and it therefore cannot provide a quantitative information about the magnetic moment change. However, the results for the Co/Pd/Cu(001) system show that the Co-Pd interaction is limited to the single atomic layers of Pd and Co forming the interface. This is in agreement with theoretical predictions of the induced magnetic moment mainly in the topmost atomic layer of the Pd(001) substrate[17] by the adjacent Co film.

The temperature dependence of the MOKE signal for 2 ML Co/1 ML Pd/Cu(001) was measured to determine the Curie temperature of the magnetic Co film—Fig. 8. Due to

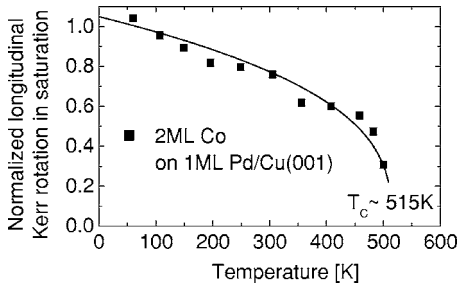

FIG. 8. Temperature dependence of Kerr rotation at saturation for 2 ML of Co on 1 ML Pd/Cu(001). Kerr rotation is normalized to the value measured at 70 K. The solid line is a result of the fit to the power-law behavior $M \sim (1-T/T_C)^{\beta}$. The best fit was obtained for $\beta=0.35$ and $T_C=515$ K.

the limit of our sample heating system the MOKE data above 500 K were fitted by extrapolating the temperature dependence of magnetization based on a power-law behavior $M \sim (1-T/T_C)^{\beta}$. The Curie temperature, T_C, of 2 ML Co/1 ML Pd/Cu(001) is 515 K. This is very close to the value for 2 ML Co/Pd(001) ($T_C \approx 560$ K), but much higher than that of 2 ML Co/Cu(001) ($T_C \approx 340$ K).[13] If Pd at the Co/Pd interface carries an induced moment due to the Co polarization,[16,17] the induced moment of Pd can enhance the T_C of the Co film. Similar T_C behavior has been found in the Fe/Pd(001) films,[36,37] where the Curie temperature of the Fe ultrathin films has shown a strong dependence on the Fe-Pd interaction.[36] Therefore, the enhanced T_C could be explained as the effect of the Co/Pd interface as well.

V. SUMMARY

The crystallographic structure, growth mode, and related morphology of Co films on Pd/Cu(001) and on Pd(001) is mainly determined by the actual interface strain. The Co/PLD-grown 1 ML Pd/Cu(001) system shows a 2D growth mode and a crystallographic long-range order even for higher Co coverage. For the Co/Pd(001) structures, the 2D growth mode has been observed up to about 2–3 ML only.

The experimental results confirmed that the slope of the Kerr rotation variation with Co thickness above ~2 ML in the Co/Cu(001), Co/Pd/Cu(001), and Co/Pd(001) structures for the same magneto-optical geometry is determined by the substrate material as expected from the electromagnetic theory.

The Kerr rotation signal from the Co/Pd systems comprises the Co-Pd interface contribution which is independent of Co thickness (above the Co thickness corresponding to the interface formation). By varying the Pd buffer thickness, it was clearly demonstrated for the Co/Pd/Cu(001) system that the Co-Pd electronic interaction occurs mainly in the single neighboring atomic layers of Pd and Co.

The Co-Pd interface contribution is much smaller in the case of the Co/Pd/Cu(001) system in comparison to the effect for the Co/Pd(001) system. Besides the different Co/Pd intermixing mechanisms in both cases, this could suggest the role of the lattice expansion of the Co overlayer for the large Co/Pd interface contribution to the total Kerr rotation signal from the Co/Pd(001) system.

ACKNOWLEDGMENTS

The authors thank X. F. Jin for helpful discussions and G. Kroder for technical support.

*Electronic address: mprzybyl@mpi-halle.mpg.de

[1] *Ultrathin Magnetic Structures I and II*, edited by B. Heinrich and J. A. C. Bland (Springer-Verlag, Heidelberg, 1994).
[2] P. Grünberg, R. Schreiber, Y. Pang, M. B. Brodsky, and H. Sowers, Phys. Rev. Lett. **57**, 2442 (1986).
[3] S. S. P. Parkin, N. More, and K. P. Roche, Phys. Rev. Lett. **64**, 2304 (1990).
[4] M. N. Baibich, J. M. Broto, A. Fert, F. Nguyen Van Dau, F. Petroff, P. Etienne, G. Creuzet, A. Friederich, and J. Chazelas, Phys. Rev. Lett. **61**, 2472 (1988).
[5] A. K. Schmid and J. Kirschner, Ultramicroscopy **42-44**, 483 (1992).
[6] P. Krams, F. Lauks, R. L. Stamps, B. Hillebrands, and G. Güntherodt, Phys. Rev. Lett. **69**, 3674 (1992).
[7] C. M. Schneider, P. Bressler, P. Schuster, J. Kirschner, J. J. de Miguel, and R. Miranda, Phys. Rev. Lett. **64**, 1059 (1990).
[8] V. S. Stepanyuk, D. I. Bazhanov, W. Hergert, and J. Kirschner, Phys. Rev. B **63**, 153406 (2001).
[9] R. Pentcheva, K. A. Fichthorn, M. Scheffler, T. Bernhard, R. Pfandzelter, and H. Winter, Phys. Rev. Lett. **90**, 076101 (2003).
[10] R. A. Miron and K. A. Fichthorn, Phys. Rev. B **72**, 035415 (2005).
[11] C. M. Schneider, A. K. Schmid, P. Schuster, H. P. Oepen, and J. Kirschner, *Magnetism and Structure in Systems of Reduced Dimensions* (Plenum Press, New York, 1992), pp. 453–466.
[12] J. Fassbender, R. Allenspach, and U. Dürig, Surf. Sci. **383**, L742 (1997).
[13] U. Bovensiepen, P. Poulopoulos, W. Platow, M. Farle, and K. Baberschke, J. Magn. Magn. Mater. **192**, 386 (1999).
[14] F. Nouvertné, U. May, M. Bamming, A. Rampe, U. Korte, G. Güntherodt, R. Pentcheva, and M. Scheffler, Phys. Rev. B **60**, 14382 (1999).
[15] P. Poulopoulos, P. J. Jensen, A. Ney, J. Lindner, and K. Baberschke, Phys. Rev. B **65**, 064431 (2002).
[16] A. Oswald, R. Zeller, and P. H. Dederichs, Phys. Rev. Lett. **56**, 1419 (1986).
[17] S. Blügel, B. Drittler, R. Zeller, and P. H. Dederichs, Appl. Phys. A **A49**, 547 (1989).
[18] Y. Wu, J. Stöhr, B. D. Hermsmeier, M. G. Samant, and D. Weller, Phys. Rev. Lett. **69**, 2307 (1992).
[19] S. K. Kim and J. B. Kortright, Phys. Rev. Lett. **86**, 1347 (2001).
[20] S. Imai, N. Inaba, H. Awano, and N. Ota, J. Appl. Phys. **97**,

10J105 (2005).
[21] T. D. Pope, G. W. Anderson, K. Griffiths, P. R. Norton, and G. W. Graham, Phys. Rev. B **44**, 11518 (1991).
[22] H. L. Meyerheim, E. Soyka, and J. Kirschner (unpublished).
[23] M. Przybylski, L. Yan, J. Zukrowski, M. Nyvlt, Y. Shi, A. Winkelmann, M. Wasniowska, J. Barthel, and J. Kirschner (unpublished).
[24] J. Fassbender, U. May, B. Schirmer, R. M. Jungblut, B. Hillebrands, and G. Güntherodt, Phys. Rev. Lett. **75**, 4476 (1995).
[25] A. R. Miedema, Z. Metallkd. **69**, 287 (1978).
[26] A. R. Miedema and F. J. A. den Broeder, Z. Metallkd. **70**, 14 (1979).
[27] J. R. Cerda, P. L. de Andres, A. Cebollada, R. Miranda, E. Navas, P. Schuster, C. M. Schneider, and J. Kirschner, J. Phys.: Condens. Matter **5**, 2055 (1993).
[28] Z. Q. Qiu, J. Pearson, and S. D. Bader, Phys. Rev. B **45**, 7211 (1992).
[29] Š. Višňovský, Czech. J. Phys. **48**, 1083 (1998).
[30] Z. Q. Qiu and S. D. Bader, J. Magn. Magn. Mater. **200**, 664 (1999).
[31] P. B. Johnson and R. W. Christy, Phys. Rev. B **6**, 4370 (1972).
[32] P. B. Johnson and R. W. Christy, Phys. Rev. B **9**, 5056 (1974).
[33] Š. Višňovský, M. Nývlt, V. Pařizek, P. Kielar, V. Prosser, and R. Krishnan, IEEE Trans. Magn. **29**, 3390 (1993).
[34] P. M. Oppeneer, in *Handbook of Magnetic Materials*, edited by K. H. J. Buschow (Elsevier, Amsterdam, 2001), Vol. 13, p. 229.
[35] Y. F. Lu, M. Przybylski, L. Yan, J. Barthel, H. L. Meyerheim, and J. Kirschner, J. Magn. Magn. Mater. **286**, 405 (2005).
[36] K. J. Strandburg, D. W. Hall, C. Liu, and S. D. Bader, Phys. Rev. B **46**, 10818 (1992).
[37] H. J. Choi, R. K. Kawakami, E. J. Escorcia-Aparicio, Z. Q. Qiu, J. Pearson, J. S. Jiang, D. Li, and S. D. Bader, Phys. Rev. Lett. **82**, 1947 (1999).